

Cite this: *J. Mater. Chem.*, 2012, **22**, 12983

www.rsc.org/materials

**Dynamic curvature control of rolled-up metal nanomembranes activated by magnesium<sup>†‡</sup>**Guojiang Wan,<sup>\*ab</sup> Alexander A. Solovov,<sup>b</sup> G. S. Huang,<sup>c</sup> Manfred F. Maitz,<sup>ad</sup> Nan Huang<sup>a</sup> and Y. F. Mei<sup>\*bc</sup>

Received 2nd February 2012, Accepted 9th May 2012

DOI: 10.1039/c2jm30641g

**Dynamic curvature control of rolled-up metal nanomembranes using an active magnesium layer design is implemented in bio-oriented conditions to realize shape transformation of expansion, shrinking, un-rolling and re-rolling. The tube integrated with a catalytic Pt layer is proposed for a new type of smart drug delivery microsystem.**

Shaped sheets or membranes on a small scale are often found in nature and play a paramount role in enabling the multi-functionalities of living systems.<sup>1</sup> This process has inspired a paradigm for creating synthetic counterparts of nano-scale thickness membranes (nanomembranes: NMs) as well as forming them into various spatial configurations (tubes, spirals, helices, wrinkles/buckles, ribbons, *etc.*). These synthetic forms, when integrated onto micro/nano-devices, could serve a vast array of potential applications<sup>2–3</sup> such as in mechanics, electronics, optoelectronics, fluidics, sensors and bio-devices to name just a few. The individual objects themselves could work in micro/nano-robotics, single-cell analysis, miniature electrodes and so on. One forming method is known as rolled-up nanotechnology, a method which causes nanofilms to self-scroll into micro/nanotubes.<sup>4,5</sup> The key process is utilizing built-in strain forces in thin solid films. Such films release from the substrates and roll up into nanomembrane micro/nanotubes (Rolled-Up Nanomembrane micro/nanoTubes: RUNTs) to relax the built-in strain,<sup>5</sup> a process known as strain engineering. The use of this process has been flourishing owing to its extraordinary traits such as well-defined 3D

tubular geometry, extremely high aspect ratio (radius-to-thickness ratio of up to 1 : 1000), and unique multi-shell and none-closed scroll structures.<sup>6–8</sup> Recently, a generic approach has been established to put forward this nanotechnology in combination with conventional photolithography and thin film vacuum deposition.<sup>6</sup> The materials' versatility and deposition compatibility make designing and producing RUNTs out of functional hybrid multi-layered nanofilms relatively easy.

Dynamic shape-control of RUNTs remains relatively unexplored and challenging,<sup>6,9,10</sup> and a simple and bio-compatible process is of course highly interesting for biological or medical applications.<sup>11</sup> In this communication, we present our conceptual design and experimental demonstration of the dynamic curvature-control of RUNTs using the active material magnesium (Mg). The curvature-control design is based on assembly, disassembly and spontaneous chemical modification of the active Mg layer on RUNTs, and is implemented by simply placing it in water, a bio-oriented condition. Our work on such processes can not only offer a strategic approach towards realistic future applications in biological or medical fields, but also help us to understand the fundamental mechanical behavior of strain-engineered NMs. Furthermore, we demonstrate how shape-tunable RUNTs with inserted catalytic layers can work as highly efficient micro/nano-engines. Such RUNTs, with integrated functionalities of engines, transformers and chemo-locomotors, offer a potential starting point for smart drug delivery systems.<sup>11</sup> For instance, Mg can be replaced with other materials, which can be removed or dissolved in certain fluids; and rolled-up engines containing active materials could release or stop releasing drugs based on expansion or contraction when meeting certain fluids.

In our experiments, bi-layer Ti and Cr nanofilms were deposited by e-beam deposition sequentially onto lithographically patterned polymer layers (AR-P3510 photoresist) on a silicon (111) substrate. The pre-stressed bi-layers were automatically rolled-up into nanomembrane tubes (RUNTs) by dissolving the photoresist layer in solvents (such as acetone or ethanol). The RUNTs were supercritical-point-dried for optical and SEM observation. All RUNTs had the same Ti/Cr (5/5 nm) bi-layer framework. Additionally, Ti/Cr/Mg (5/5/5–20 nm) RUNTs with active Mg on top were prepared for expansion and contraction control in water. Ti/Cr/Mg (5/5/10 nm) trilayers were taken freshly out of the vacuum and placed into acetone for scrolling and remained in the acetone for a relatively long time (approx. 45 min) for surface chemical modification of Mg by reaction with the acetone. Then the rolled-up RUNTs were instantly

<sup>a</sup>Key Lab. of Advanced Technologies of Materials, Ministry of Education, College of Materials Science and Engineering, Southwest Jiaotong University, 610031 Chengdu, P. R. China. E-mail: guojiang.wan@home.swjtu.edu.cn

<sup>b</sup>Institute for Integrative Nanosciences, IFW Dresden, Helmholtzstr. 20, 01069 Dresden, Germany

<sup>c</sup>Department of Materials Science, Fudan University, Handan Road 220, 200433 Shanghai, P. R. China. E-mail: yfm@fudan.edu.cn

<sup>d</sup>Leibniz Institute of Polymer Research Dresden, Max Bergmann Center of Biomaterials Dresden, 01097 Dresden, Germany

<sup>†</sup> Electronic supplementary information (ESI) available. See DOI: 10.1039/c2jm30641g

<sup>‡</sup> This work is financially supported by the Sichuan Youth Science and Technology Foundation (No.2012JQ0001) for Distinguished Young Scholars, the China Scholarship Council (CSC), and the National Natural Science Foundation of China (no. 20973134, no. 20603027 and no. 61008029), Shishi star program of SWJTU and "Shu Guang" project by Shanghai Municipal Education Commission and Shanghai Education Development Foundation.

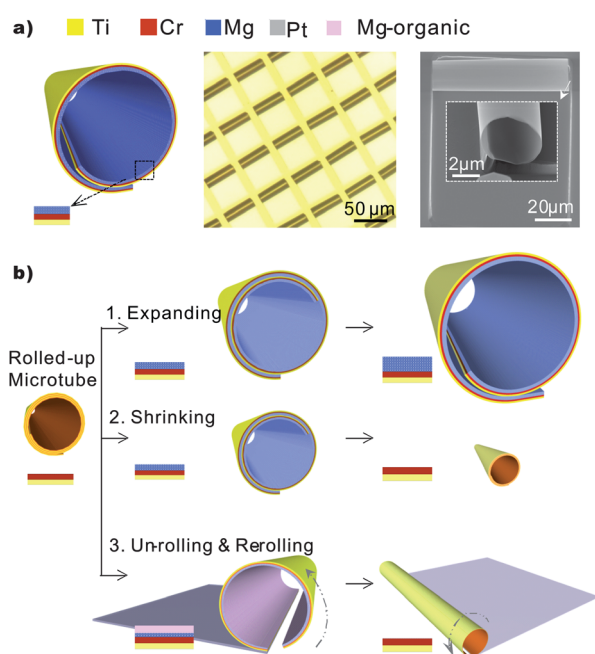
transferred into water for observation of the dynamic motions of un-rolling, re-rolling and shrinking under an optical microscope with a high-speed camera (Photonic Science Limited); images were captured by the live videos at 50 frames per second. A very thin Pt layer (0.5 nm) was inserted into the Ti/Cr/Mg tri-layer underneath the Mg by sputtering deposition to produce Ti/Cr/Pt/Mg (5/5/0.5/10 nm) RUNTs as catalytic micro/nano engines (N-jets). The N-jets were detached from the Si substrate into hydrogen peroxide solutions (from 0.1 to 10 wt%) with surfactant (0.5 wt% benzalkonium chloride), and were then observed using the above-mentioned optical microscope and camera. The contact angle was measured by Data-Physics equipment (OCA series) on the samples of Ti film, and the surface produced by Mg-mediated reaction (deposited Mg film immersed instantly in acetone for 45 min then critical point dried).

In order to realize dynamic curvature-control of our RUNTs, we create a functional strain-engineered bi-layer for roll-up and an active layer for curvature-tuning. As sketched in Fig. 1, a Ti/Cr (titanium/chromium) bi-layer provides a basic rolling framework because of the two materials' readily available stress misfit for scrolling. The Ti and Cr nanofilms are subsequently deposited onto a patterned photoresist layer (as a sacrificial layer) on a silicon substrate, with a material beam incidence angle (the angle between the orientation of the sample surface and the direction of deposited material flux), here  $60^\circ$ , for shadowing one side wall to create an etch window.<sup>6</sup> By etching away patterns through the shadowed side, Ti/Cr nanofilms curl up spontaneously to relax the mismatched stress, and eventually roll up into RUNTs with multiple windings (rotations). As for the curvature control, we adopt Mg as an active layer due to its unique physical and chemical properties as well as unquestionable safety in biomedical applications. The active Mg layer is topped onto a Ti/Cr bi-layer with

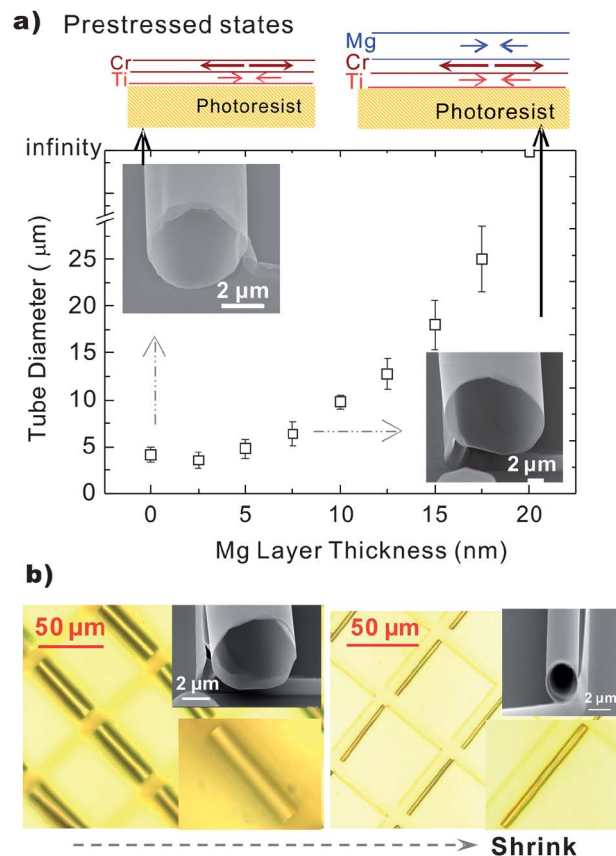
appropriate thicknesses as illustrated in the left image of Fig. 1a. Ti/Cr/Mg tri-layered RUNTs are then formed with high yield (see the middle image of Fig. 1a). An individual tube displays a well-shaped scroll structure with tightly bonded windings as shown in the right-hand image of Fig. 1a. Consequently, dynamic curvature-control (for example, expanding, shrinking, unrolling and re-rolling) can be realized using Mg-activated RUNTs as depicted in Fig. 1b: (1) assembly/deposition of an active Mg layer leads to expansion of Ti/Cr RUNTs in diameter by a physico-mechanical mediation of the pre-stress states across the whole NMs; (2) disassembly/degradation of an Mg layer in water causes RUNTs to shrink in diameter; (3) surface modification of the Mg layer with acetone and/or water could enable RUNTs to un-roll and then re-roll in a dynamic evolution.

Fig. 2 shows that the diameter of Ti/Cr RUNTs can be effectively increased by thickening the Mg top-layer of Ti/Cr/Mg tri-layer NMs. These NMs roll up into expanded RUNTs with an increased thickness equal only to that of the Mg layer. However, such nano-membranes remain uncurled when Mg thickness reaches and exceeds approx. 20 nm (Fig. 2a). Note that the Ti/Cr thickness (5/5 nm) remains constant and the change of the curvature is attributed solely to the added Mg layer.

It is known that the curvature of RUNTs depends on the pre-stress mismatch across all of the layers, as well as the layer thickness itself.<sup>4,5</sup>



**Fig. 1** Scheme of curvature-control RUNTs by active Mg design: (a) left: active Mg on Ti/Cr framed RUNTs; middle: representative optical microscope image of RUNTs (Ti/Cr/Mg, 5/5/10 nm); right: SEM graphs of individual tubes. (b) Dynamic curvature-control: (1) expansion by active Mg assembly; (2) shrinking by Mg layer disassembly; (3) *in situ* un-rolling and re-rolling by chemical and physico-chemical interaction.



**Fig. 2** Shape control of RUNTs by assembly and disassembly of Mg layer: (a) expansion by Mg assembly: diameter increase of RUNTs with Mg thickness (Ti/Cr/Mg, 5/5/0–20 nm), and upper: illustration of pre-stress states across the total NMs; (b) shrinking by Mg disassembly: optical and SEM images of, left: as-rolled-up RUNTs Ti/Cr/Mg (5/5/10 nm) and right: shrunken RUNTs in water.

The pre-stress in each layer originates mainly from thermal and intrinsic residual stresses.<sup>12</sup> For instance, a Cr film deposited at room temperature has a high tensile residual stress because of its low  $T_d/T_m$  ( $T_d$ : deposition temperature,  $T_m$ : melting point; leading to low atom mobility), its body-centered-cubic crystalline type and structural flaws; while a Ti film deposited under the same conditions presents a comparably compressive state due to its relatively high  $T_d/T_m$  as well as its hexagonal structure.<sup>12,13</sup> Hence, such stress differences between Ti and Cr layers are responsible for the curling phenomenon once the whole bi-layer releases from the substrate (the upper left panel in Fig. 2a). When topped with one Mg layer, the whole Ti/Cr/Mg tri-layer can develop one modified stress-state across the total NM. Mg has different physical and mechanical properties compared with Ti and Cr, such as a higher thermal expansion coefficient ( $25.0, 6.2, 8.6 \mu\text{m}\cdot\text{m}^{-1}\cdot\text{K}^{-1}$  for Mg, Cr, Ti respectively<sup>12</sup>), higher  $T_d/T_m$  than Cr and Ti, and its unique hexagonal closed-pack (HCP) crystallographic structure. All these features cause the deposited Mg layer to build up a higher compressive stress state compared with the underlying Ti/Cr layers.<sup>12,13</sup> Thus, as depicted in the upper right panel of Fig. 2a, the Mg layer effectively offsets the tensile stress built up in the Cr layer and therefore reduces the driving force for curling up. But with a very thin Mg layer things get more complicated, most likely due to other surface effects such as coalescence, roughness, *etc.*<sup>13</sup> It is worth noting that beyond the offsetting caused by the Mg layer, the thickness of the NM itself can also result in an increase in the diameter (scaling up) of the rolled-up tubes,<sup>6,14</sup> but the offsetting effect described above seems to dominate our rolling system. An additional Mg layer with a neutral/tensile strain state can smoothly increase or decrease the diameter of the tube, but will not entirely stop the rolling-up process. In our system, a 20 nm-thick Mg layer can stop the rolling of the whole NM. This shows that strain mismatch is mainly responsible for the scaling up of our RUNTs.

The dynamic shape-control of micro/nanoscale objects is of fundamental significance in nature and artificial structures.<sup>15-17</sup> Thurmer *et al.* found that the dissolution of an  $\text{Nb}_2\text{O}_5$  layer could readjust the strain gradient in the whole layer and thus change the rolling behaviour.<sup>16</sup> Here, the active Mg material on our RUNTs can fulfill the task of dynamic curvature control without any external forces, because it can simply dissolve in water. We prepared Ti/Cr/Mg RUNTs (5/5/10 nm) and found that they can shrink dynamically in water by a significant amount (from approx. 11  $\mu\text{m}$  to approx. 2  $\mu\text{m}$  in diameter) after the Mg layer is dissolved away. Strikingly, the shrunken tubes become even smaller than normal Ti/Cr bi-layer RUNTs with the same thickness (approx. 5.5  $\mu\text{m}$ ). The reasons hypothesized are thus: firstly, the dynamically reducing thickness causes lower stiffness of NMs and therefore easier bending/curling. Secondly, hydrogen bubbles produced on the inner wall of the Mg layer when it dissolves result in a compression effect as well as extra gas/solid surface tension, leading to further shrinking.<sup>18</sup> Likewise, the hydrogen bubbles and *in situ* Mg dissolving during the shrinking process are likely to prevent neighboring windings from bonding simultaneously, also contributing to the reduced RUNT diameter.

Expanding and shrinking RUNTs by assembly and disassembly of an active layer has proven an effective method to tune the curvature of rolled-up NMs without any additional external forces. Using a similar process, surface modification of the active layer can also be used to change the chemo-mechanical properties of its surface. Fast responses and simple processes may make such treatment an efficient way to assemble and/or disassemble micro/nano-architectures. Here,

we placed the deposited NMs (Ti/Cr/Mg, 5/5/10 nm) into acetone (also as an etching solution for the sacrificial layer), and observed the results. The NMs rolled up into RUNTs, and at the same time the active Mg reacted with the acetone to form a chemically modified layer. After about 45 minutes' reaction time, we transferred the rolled-up RUNTs instantly into water. Surprisingly, we found that the RUNTs displayed a dynamic curvature change. As demonstrated in Video S1† and the captured images in Fig. 3a, the RUNTs unrolled first, then re-rolled back into tubes again, and finally shrank to become smaller RUNTs.

The rationale for the un-rolling process is sketched in Fig. 3b. It is proposed that an intermediate organometallic product was formed firstly on the top layer when the active Mg reacted with the acetone (Fig. 3c) by a pinacol coupling reaction (Grignard chemical reaction) due to the Mg's extremely high reactivity.<sup>19</sup> In order to prove such an assumption, the modified surface was measured as being hydrophobic (Fig. 3b, left lower inset) using the water contact angle method on pre-prepared films after a prolonged reaction in acetone; while the opposite outer Ti layer still remained hydrophilic (Fig. 3b, right upper inset). The hydrophilicity imbalance between the inner Mg and outer Ti layers is the direct cause of the asymmetry in surface tension illustrated in Fig. 3b.<sup>18</sup> The interfacial/surface tension induces a compressive force on the outermost solid surface to counter against attractive forces among water molecules.<sup>18</sup> Evidently, the magnitude of the interfacial force upon the hydrophilic Ti layer is substantially larger than that on the hydrophobic modified Mg-organic layer, hence producing an unfolding outwards force. Quantitatively, if the surface-tension-driven momentum herein is sufficient to overcome the bending energy (mostly stored elastic energy) plus bonding energy between neighboring wings, RUNTs will un-scroll into flattened NMs in order to thermodynamically lower the energy states of the NM forms.<sup>14,20,21</sup> Such phenomena related to surface-tension-driven shape/conformational change of NMs work widely in nature and play a crucial role in implementing multi-functionalities.<sup>21</sup> For instance, cell movements/motions can be actuated through cell-membrane shape change due to hydrophilic/hydrophobic mediation

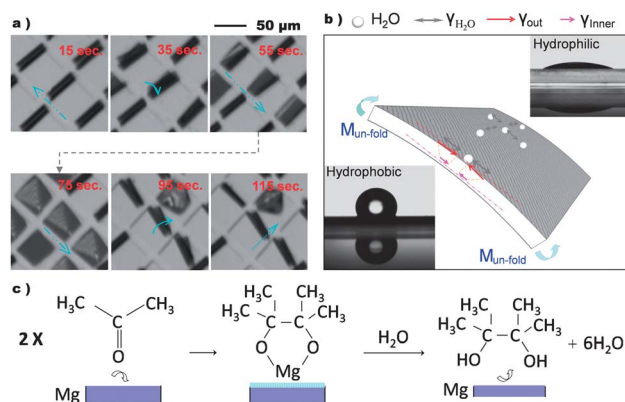


**Fig. 3** *In situ* dynamic shape-control of RUNTs: (a) un-rolling, re-rolling and shrinking frame images of RUNTs Ti/Cr/Mg(5/5/10 nm) (rolled up and chemically reacted in acetone for 45 min and then transferred instantly into water); (b) schematic rationale for un-rolling motion: unfold momentum produced by interfacial tension asymmetry between outside and inside top-layers, and optical images of: contact angle of the water on the Ti (upper right) layer, and the Mg-mediated product layer (lower left); (c) Mg reacts with acetone by pinacol coupling reaction and water by re-arrangement reaction.

by trans-membrane proteins. Similar behaviors have been consistently reported on synthetic NMs both theoretically<sup>15</sup> and experimentally,<sup>16</sup> for example the curling up of graphene sheets caused by the application of water droplets. More importantly, our success regarding such shape-control on well-defined synthetic RUNTs shows another route towards realizing smart environment-responsive NM-based objects. For example, once the Mg-organic product and then the Mg are dissolved away with water by the pinacol rearrangement reaction (Fig. 3c),<sup>19</sup> the NMs immediately re-scroll back into tubes driven solely again by the stored elastic bending energy, and finally shrink into smaller Ti/Cr bi-layer tubes in a similar way to those described above. Interestingly, the NMs re-roll back in a different direction (perpendicular to the unroll direction), which could be due to the different mechanical property of each layer in the NMs.<sup>22</sup> Also, the speed of the rolling back is much faster than that of the unrolling in the NMs, which is similar to the previous result.<sup>16</sup>

Furthermore, we demonstrate that our shape-controllable RUNTs can be applied as catalytic micro/nanoscale motors for smart drug delivery when we insert a thin catalytic material (platinum, Pt) underneath the Mg layer. The hybrid NMs (Ti/Cr/Pt/Mg, 5/5/0.5/10 nm) can roll up into tubes to perform not only the above-mentioned shape motions, but also perform as micro/nano-machines by harnessing chemical energy after the active Mg bio-degrades. This series of motions could serve for intelligent drug delivery tasks in a human-body-environment-responsive way which is a critical requirement for advanced nano-medicine.<sup>11</sup> For example, the Ti/Cr/Pt/Mg RUNTs could employ Mg to perform expanding, shrinking, un-rolling and re-

rolling for dynamic drug loading and unloading. Then, after the removal of the Mg, the drug-loaded RUNTs could move as micro/nano-engines by using Pt as a catalytic layer. Fig. 4 shows how the tubular engines run after the Mg dissolves away in H<sub>2</sub>O<sub>2</sub> solution (with 0.5 wt% surfactant of benzalkonium chloride). The H<sub>2</sub>O<sub>2</sub>-fueled chemo-locomotor is propelled by the recoiling of oxygen bubbles (produced by H<sub>2</sub>O<sub>2</sub> decomposition).<sup>6</sup> Interestingly, the tubular engines start moving noticeably at very low H<sub>2</sub>O<sub>2</sub> concentrations (0.1 wt% to 3.0 wt%, consistent with certain human body conditions<sup>24</sup>). Their linear velocity as well as body length velocity both increase with increased H<sub>2</sub>O<sub>2</sub> concentrations (Fig. 4b), reaching approx. 845  $\mu\text{m s}^{-1}$  (11.2 body lengths per second), an unrivaled speed compared with similar counterparts reported at 3.0 wt% H<sub>2</sub>O<sub>2</sub>.<sup>6,17,23</sup> Ultimately smart engines could be created to travel along H<sub>2</sub>O<sub>2</sub> gradients and target specific disease sites where there exist unusually high H<sub>2</sub>O<sub>2</sub> concentrations from the production of oxidative radicals by inflammatory/abnormal cells.

It is noteworthy that this remarkable behavior is attributed to our unique shrunken RUNTs' structure *i.e.* their loosely packed tubular shape. Fig. 4a (left: schematic; right SEM image) shows the tubular engines. Besides the scaling-down of the RUNTs in diameter (from approx. 11  $\mu\text{m}$  into approx. 2  $\mu\text{m}$ ), even more importantly, the inner part appears much looser and many neighboring windings are not tightly bonded with each other. All these exposed inner areas act as catalytic reaction surfaces for oxygen bubble production. Note that the diameter of the central tubular aperture reaches a scale of approx. 800 nm. The greater number of exposed surfaces can result in enhanced H<sub>2</sub>O<sub>2</sub> chemical decomposition caused by the Pt catalyst; while the face-to-face Pt and Ti in H<sub>2</sub>O<sub>2</sub> electrolyte solution act as bimetallic galvanic cells and can therefore also accelerate H<sub>2</sub>O<sub>2</sub> electrochemical decomposition.<sup>17,23</sup> Both features may favor the increase of H<sub>2</sub>O<sub>2</sub> decomposition into oxygen bubbles. Thus our shrunken tubular engines can lead to bubble generation with a higher frequency compared with other engines.<sup>17,23</sup>

## Conclusions

In conclusion, we have demonstrated dynamic curvature-control of rolled-up nanomembrane tubes in biocompatible environments through active Mg layer designs. Combined with catalytic Pt, the hybrid tubes can function as micro/nano-engines and implement a series of spontaneous motions in a human body environment without the need for external forces. The dynamic shape changes, together with H<sub>2</sub>O<sub>2</sub> trace responsive chemo-locomotion, could help our RUNTs to serve directly as smart drug delivery systems.<sup>25</sup> Interesting future work may focus on completing the intelligent *in vitro* or *in vivo* tasks highly demanded in nano-biomedicine, such as drug loading, delivery, targeting and attacking. Moreover, such concepts also provide vast possibilities for creating new types of environmentally responsive intelligent nanomembrane-based objects, designed for diverse applications such as bio/chemo-sensors, detectors, scavengers and robots at a micro/nano-scale.<sup>26</sup> The science revealed therein can also help us to better understand both our natural and synthetic worlds.<sup>1,27,28</sup>

## Notes and references

- M. M. Kozlov, *Nature*, 2010, **463**, 439; H. T. McMahon and J. L. Gallop, *Nature*, 2005, **438**, 590; Y. Shibata, J. Hu, M. M. Kozlov and T. A. Rapoport, *Annu. Rev. Cell Dev. Biol.*,

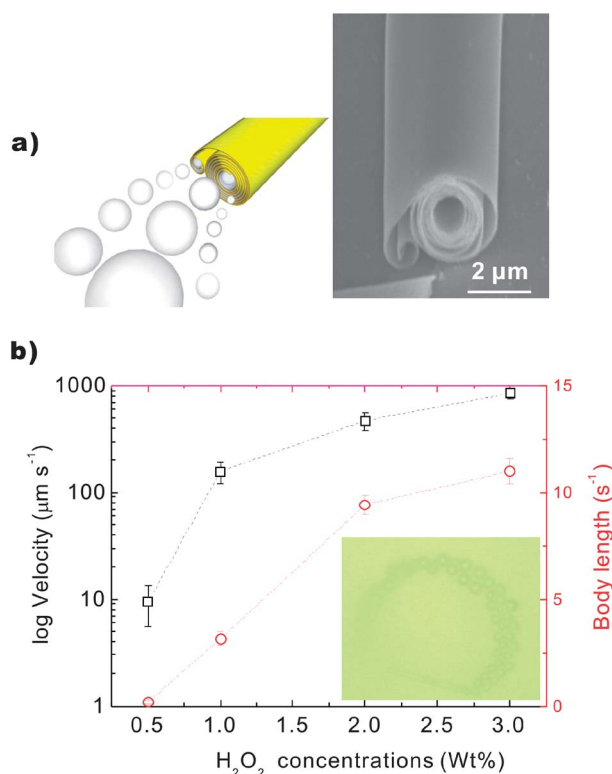


**Fig. 4** Pt inserted Mg-based RUNTs (Ti/Cr/Pt/Mg, 5/5/0.5/10 nm) as nano-engines (jets) in H<sub>2</sub>O<sub>2</sub> solution: (a) schematic (left) and SEM micrograph (right) of N-engine, and (b) translocation speed (linear velocity and body length) with H<sub>2</sub>O<sub>2</sub> concentrations, and the representative optical image of moving N-jets (inset).

- 2009, **25**, 329; Y. Yu, J. A. Vroman, S. C. Bae and S. J. Granick, *J. Am. Chem. Soc.*, 2010, **132**, 195.
- 2 W. T. Huck, A. D. Stroock and G. M. Whitesides, *Angew. Chem., Int. Ed.*, 2000, **39**, 1058; G. M. Whitesides, *Small*, 2005, **1**, 172; R. Vendamme, S. Y. Onoue, A. Nakao and T. Kunitake, *Nat. Mater.*, 2006, **5**, 494.
- 3 W. L. Cheng, M. J. Campolongo, S. J. Tan and D. Luo, *Nano Today*, 2009, **4**, 482; J. A. Rogers, T. Someya and Y. G. Huang, *Science*, 2010, **327**, 1603; Y. F. Mei, S. Kiravittaya, M. Benyoucef, D. J. Thurmer, T. Zander, C. Deneke, F. Cavallo, A. Rastelli and O. G. Schmidt, *Nano Lett.*, 2007, **7**, 1676; T. J. Kanga, D. K. Limb, J. M. Namb and Y. H. Kim, *Sens. Actuators, B*, 2010, **147**, 691; D.-H. Kim and J. A. Rogers, *ACS Nano*, 2009, **3**, 498; M. Grundmann, *Phys. Status Solidi B*, 2010, **247**, 1257.
- 4 V. Y. Prinz, V. A. Seleznev, A. K. Gutakovskiy, A. V. Chehovskiy, V. V. Preobrazhenskii, M. A. Putyato and T. A. Gavrilova, *Phys. Rev. E: Stat. Phys., Plasmas, Fluids, Relat. Interdiscip. Top.*, 2000, **6**, 828.
- 5 O. G. Schmidt and K. Eberl, *Nature*, 2001, **410**, 168; O. G. Schmidt, N. Schmarje, C. Deneke, C. Müller and N.-Y. Jin-Phillipp, *Adv. Mater.*, 2001, **13**, 756; O. G. Schmidt, N. Y. Jin-Phillipp, C. Lange, U. Denker, K. Eberl, R. Schreiner, H. Gräbeldinger and H. Schweizer, *Appl. Phys. Lett.*, 2000, **77**, 4139.
- 6 Y. F. Mei, G. S. Huang, A. A. Solovev, E. B. Urena, I. Moench, F. Ding, T. Reindl, R. K. Y. Fu, P. K. Chu and O. G. Schmidt, *Adv. Mater.*, 2008, **20**, 4085; Y. F. Mei, A. A. Solovev, S. Sanchez and O. G. Schmidt, *Chem. Soc. Rev.*, 2011, **40**, 2109.
- 7 G. S. Huang, Y. F. Mei, D. J. Thurmer, E. Coric and O. G. Schmidt, *Lab Chip*, 2009, **9**, 263.
- 8 A. Cho, *Science*, 2006, **313**, 164.
- 9 E. Smela, O. Inganas and I. Lundstrom, *Science*, 1995, **268**, 1735.
- 10 J. S. Randhawa, M. D. Keung, P. Tyagi and D. H. Gracias, *Adv. Mater.*, 2010, **22**, 407; J. H. Cho, T. James and D. H. Gracias, *Adv. Mater.*, 2010, **22**, 2320; J. H. Cho and D. H. Gracias, *Nano Lett.*, 2009, **9**, 4049; J. S. Randhawa, T. G. Leong, N. Bassik, B. R. Benson, M. T. Jochmans and D. H. Gracias, *J. Am. Chem. Soc.*, 2008, **130**, 17238.
- 11 T. M. Allen and P. R. Cullis, *Science*, 2004, **303**, 1818.
- 12 L. B. Freund and S. Suresh, *Thin Film Materials: Stress, Defect Formation and Surface Evolution*, Cambridge University Press, New York, 2009, The ralted information can be also found at <http://www.engineeringtoolbox.com>.
- 13 Y. C. Tsui and T. W. Clyne, *Thin Solid Films*, 1997, **306**, 23; C. H. Hsueh, *Thin Solid Films*, 2002, **418**, 182; T. D. Moore and J. L. Jarvis, *Microelectron. Reliab.*, 2003, **43**, 487.
- 14 P. Cendula, S. Kiravittaya, Y. F. Mei, C. Deneke and O. G. Schmidt, *Phys. Rev. B: Condens. Matter Mater. Phys.*, 2009, **79**, 085429; C. Deneke, C. Müller, N. Y. Jin-Phillipp and O. G. Schmidt, *Semicond. Sci. Technol.*, 2002, **17**, 1278; Ch. Deneke, N.-Y. Jin-Phillipp, I. Loa and O. G. Schmidt, *Appl. Phys. Lett.*, 2004, **84**, 4475.
- 15 J. Zang, M. H. Huang and F. Liu, *Phys. Rev. Lett.*, 2007, **98**, 146102; N. Patra, B. Y. Wang and P. Kral, *Nano Lett.*, 2009, **9**, 3766.
- 16 D. J. Thurmer, C. Deneke and O. G. Schmidt, *J. Phys. D: Appl. Phys.*, 2008, **41**, 205419.
- 17 W. F. Paxton, S. Sundararajan, T. E. Mallouk and A. Sen, *Angew. Chem., Int. Ed.*, 2006, **45**, 5420; W. F. Paxton, P. T. Baker, T. R. Kline, Y. Wang, T. E. Mallouk and A. Sen, *J. Am. Chem. Soc.*, 2006, **128**, 14881; K. K. Dey, B. R. Panda, A. Paul, S. Basu and A. Chattopadhyay, *J. Colloid Interface Sci.*, 2010, **348**, 335.
- 18 L. I. Trakhtenberg, S. H. Lin and O. J. Ilegbusi, *Physico-Chemical Phenomena in Thin Films and at Solid Surfaces* (Thin Films and Nanostructures), Academic Press, 1st edn, 2007, vol. 34.
- 19 C. J. Li and W. C. Zhang, *J. Am. Chem. Soc.*, 1998, **120**, 9102; W. C. Zhang and C. J. Li, *J. Org. Chem.*, 1999, **64**, 3230; C. J. Li, *Chem. Rev.*, 2005, **105**, 3095.
- 20 G. Stoney, *Proc. R. Soc. London, Ser. A*, 1909, 82; J. Mattsson, J. A. Forrest and L. Borjesson, *Phys. Rev. E: Stat. Phys., Plasmas, Fluids, Relat. Interdiscip. Top.*, 2000, **62**, 5187.
- 21 T. R. Graham and M. M. Kozlov, *Curr. Opin. Cell Biol.*, 2010, **22**, 430; F. Campelo, H. T. McMahon and M. M. Kozlo, *Biophys. J.*, 2008, **95**, 2325; J. Zimmerberg and M. M. Kozlov, *Nat. Rev. Mol. Cell Biol.*, 2006, **7**, 9.
- 22 W. M. Li, G. S. Huang, J. Wang, Y. Yu, X. J. Wu, X. G. Cui and Y. F. Mei, *Lab Chip*, 2012, DOI: 10.1039/c2lc40151g.
- 23 A. A. Solovev, Y. F. Mei and O. G. Schmidt, *Adv. Mater.*, 2010, **22**, 4340; A. A. Solovev, Y. F. Mei, E. Bermúdez Ureña, G. S. Huang and O. G. Schmidt, *Small*, 2009, **5**, 1688; A. A. Solovev, S. Sanchez, M. Pumera, S. Schulze, Y. F. Mei and O. G. Schmidt, *Adv. Funct. Mater.*, 2010, **20**, 2430.
- 24 B. Halliwell, M. V. Clement and L. H. Long, *FEBS Lett.*, 2000, **486**, 10.
- 25 M. Murakami, H. Cabral, Y. Matsumoto, S. Wu, M. R. Kano, T. Yamori, N. Nishiyama and K. Kataoka, *Sci. Transl. Med.*, 2011, **3**, 64ra2; L. Liu, W. Wang, X. J. Ju, R. Xie and L. Y. Chu, *Soft Matter*, 2010, **6**, 3759; M. S. Yavuz, Y. Cheng, J. Chen, C. M. Cobley, Q. Zhang, M. Rycenga, J. Xie, C. Kim, K. H. Song, A. G. Schwartz, L. V. Wang and Y. Xia, *Nat. Mater.*, 2009, **8**, 935.
- 26 G. S. Huang and Y. F. Mei, *Adv. Mater.*, 2012, **24**, 2517.
- 27 K. K. Dey, B. R. Panda, A. Paul, S. Basu and A. Chattopadhyay, *J. Colloid Interface Sci.*, 2010, **348**, 335; D. L. Hu and J. W. M. Bush, *Nature*, 2003, **424**, 663; X. Gao and L. Jiang, *Nature*, 2004, **432**, 36; L. Jiang, X. Yao, H. Li, Y. Fu, L. Chen, Q. Meng, W. Hu and L. Jiang, *Adv. Mater.*, 2010, **22**, 376.
- 28 A. E. Nel, L. Mädler, D. Velegol, T. Xia, E. M. V. Hoek, P. Somasundaran, F. Klaessig, V. Castranova and M. Thompson, *Nat. Mater.*, 2009, **8**, 543.